Refinery Wastewater Treatment by a Novel Three-Dimensional Electrocoagulation System Design

Samar K. Theydan
Department of Chemical Engineering
College of Engineering, University of Baghdad
Baghdad, Iraq
samar.kareem@coeng.uobaghdad.edu.iq

Wadood Taher Mohammed
Department of Chemical Engineering
College of Engineering, University of Baghdad
Baghdad, Iraq
dr.wadood@coeng.uobaghdad.edu.iq

Abstract-A novel three-dimensional electrocoagulation method was used in the current work to explore the treatment of refinery wastewater. Metal-Impregnated Granular Activated Carbon (MIGAC) was employed as a third particle electrode in the inventive design. A comprehensive investigation has been conducted to evaluate its performance. BET-specific surface area, total pore volume, X-ray Fluorescence (XRF), Energy-Dispersive X-ray spectroscopy (EDS), and Scanning Electron Microscopy (SEM) were employed for the characterization of MIGAC particle electrodes at pH=7, 30V applied voltage, 10g of particle electrodes, 175mL/min flow rate, and a supporting electrolyte (0.063M NaCl + 0.025M Na_2SO_4). The findings indicate that the effectiveness of Chemical Oxygen Demand (COD) elimination increased quickly after 20min to 66.93, 69.88, 77.59, 74.14, 81.26, 79.87, and 87.14% for Conventional Electrocoagulation (CEC). Three-dimensional electrocoagulation with granular activated carbon (TEC-RGAC), TEC-MIGAC (Al), TEC-MIGAC (Fe), and TEC-MIGAC (Al:Fe) with molar ratios of (1:1), (1:2), and (2:1) respectively were utilized. While turbidity removals were 99.04, 98.87, 99.23, 94.89, 92.42, 98.85, and 99.21% for CEC ,TEC-RGAC, TEC-MIGAC(Al), TEC-MIGAC(Fe), TEC-MIGAC(1:1), TEC-MIGAC(1:2), and TEC-MIGAC(2:1) respectively. The results demonstrated that the metal impregnation of GAC is an interesting method for achieving effective turbidity and COD removal from refinery wastewater. In both batch and repeat recycling tests, MIGAC with a mixture of aluminum and iron oxides removed turbidity and COD more effectively and efficiently than RGAC.

Keywords-electrocoagulation; refinery wastewater; three-dimensional electrode; metal impregnated activated carbon; COD

I. INTRODUCTION

The aquatic environment is contaminated from sewage disposal, runoff from agricultural lands, air fallout, and waste management operations, such as the discharge of effluents from oil refining [1]. Refining processes convert crude oil into petroleum and other valuable byproducts. Large amounts of water are consumed throughout those activities, resulting in a proportional amount of wastewater, which consists of cooling water, process water, storm water, and sewage [2]. It was found that the amount of wastewater was about 0.4–1.6 times the amount of processed oil. In the wastewater from refineries and petrochemical plants, there are more than 20 different types of

harmful chemicals, even though the contaminants in wastewater depend a lot on the way the process is set up. Wastewater treatment structure, operational processes, and the kind of processed oil have significant impact on the composition of refinery wastewater [3]. Suspended particles, biodegradable and refractory organics, hydrocarbons, sulfides, phenols, and nitrogen compounds are the main pollutants in these industrial wastewaters [4].

As a fundamental requirement, the quality and availability of water are very important [5, 6]. Untreated effluent discharge needs to be under safety regulations [7]. So, effective and practical wastewater treatment methods for petroleum refineries are necessary. Biodegradation [8, 9], ultrafiltration [10], adsorption [11], and coagulation [12] are some of these processes. The techniques used in electrochemical processes include electroflotation (EF) [13], Electro-fenton Oxidation (EO) [14], electrocoagulation (EC) [12], and sequential EC and EO processes [15]. They have the benefits of being simply spread and requiring the least quantity of chemicals. Many studies during the recent years have focused on EC, an effective procedure for treating finely dispersed wastewater. Because this technology is both sturdy and small, it has the potential to replace complicated procedures that need huge volumes and/or a variety of chemicals [16]. Several parameters might be utilized to monitor the wastewater from petroleum refineries. One of them is the Chemical Oxygen Demand (COD), which needs comparatively less time and may be used to evaluate the water quality as a whole [17].

Electrochemical methods have showed substantial practicality in the treatment of many industrial wastewaters, such as refinery wastewater [18, 19], due to their unique capacity to oxidize or remove contaminants in the water near the properly maintained electrode. However, due to its low current density, the conventional electrochemical approach does not perform successfully throughout the wastewater treatment process [20].Complex chemical and physical changes occur often during any EC process. Positive ionic coagulants are generated as a result of sacrificial anode oxidation when a direct current or voltage is supplied. As a result of the water reduction at the cathode, hydroxyl ions (OH^-) and some O_2 and H_2 gas bubbles can be generated [21]. To eliminate

contaminants, EC depends on the electrochemical formation of metal ions such as aluminum and ferric iron, which act as stabilizing reagents and neutralize the electric charge. The isomeric replacement of ferric ions by aluminum ions in iron oxides breaks crystallization, resulting in a greater surface area of the total adsorbents (oxide minerals), which may increase the removal effectiveness during combined EC using aluminum and ferric electrodes [22]. Traditional EC approaches for water and wastewater treatment have frequently employed single electrodes such as ferric-ferric and aluminum-aluminum, or combination electrodes such as aluminum-ferric or ferric-aluminum, known as the two-dimensional electrode system [23]. Combinations of aluminum-ferric or ferric-aluminum electrodes have been proved to be more successful in removing impurities than single electrode systems [24].

The use of three-dimensional electrodes in combination with carbon particles has been proposed as an alternative method that may effectively improve the working electrode's specific surface area and has been used for the removal of chloramphenicol [25], metal ions [26], and cyanides [27] from wastewater, and recently the elimination of organic pollutants, such as phenols [28], dyes [29, 30], tetracycline [31], and furfural degradation [32].

Three-dimensional (3D) electrode-based electrochemical techniques have attracted a lot of attention. A particle electrode or bed electrode serves as a third electrode in 3D electrochemical methods, in addition to the two electrodes used in the traditional (two-dimensional) electrochemical systems. These particle electrodes are loaded between the anode and the cathode. In 3D electrochemical systems, granular or powdery materials are often utilized as the working electrode and as particle electrodes. When external potential is present, this particle microelectrode generates charge. Depending on the kind of electrode, the degradation of organic pollutants can occur in a variety of ways. In addition to the procedure in two dimensional electrochemical systems, the fabrication of microelectrodes in 3D electrochemical systems enhances pollutant degradation [33]. Additionally, active carbon, a particle electrode that is frequently used, encourages the electro-generation of hydrogen peroxide and the subsequent production of hydroxyl radicals [34]. Reduced energy consumption due to a higher surface area to volume ratio, enhanced mass transfer, increased pollutant removal efficiency, generation of additional oxidants, and elimination of pollutants by sorption on particle electrodes are the major properties of 3D electrode reactors [35, 36].

The main objective of this study is to create a Three dimensional Electrocoagulation Metal-Impregnated Granular Activated Carbon with a (TEC-MIGAC) system using metal (aluminum, iron, or both). This system was developed with the goal of using metal-impregnated carbon particles as an adsorbent and metal-support media by leveraging the collaborative action of aluminum and ferric ions. It was tested in treating wastewater from the Iraq's Al-Daura petroleum refinery facility. MIGAC's textural characteristics were studied using BET, XRF, EDS, and SEM, while COD removal, turbidity removal, Total Dissolved Solids (TDS) removal, current efficiency, and energy consumption were measured.

II. MATERIALS AND METHODS

A. Materials

The untreated petroleum refinery effluent sample (80L) was provided by the Al-Daura refinery petroleum refinery plant, Baghdad, Iraq. It was taken from the feeding tank and was stored in covered containers at $4^{o}C$ until use. Table I lists the characteristics of this sample. Because raw water's conductivity is very low, it raises the cell potential, which necessitates the addition of supportive electrolytes in order to boost conductivity. Na_2SO_4 at 3.5g/L and NaCl at 2.5g/L were employed as supporting electrolytes, which resulted in a conductivity of $12.16mScm^{-1}$, which is within the range necessary to achieve low cell potential [37].

TABLE I.   PROPERTIES OF THE UTILIZED EFFLUENT SAMPLE

Property	Value
pH (-)	6.8
COD (ppm)	1400
Conductivity (mS/cm)	2.66
Turbidity (NTU)	227
TDS g/L	6.64
F^{-} (ppm)	0.19
Cl^{-}(ppm)	422.4
Zn-(ppm)	0.08
Cu (ppm)	0.025
Mn (ppm)	0.33
Ni (ppm)	0.5

A commercial GAC was used with the physical properties shown in Table II. A mixture of anhydrous sodium sulphate (Na_2SO_4) powder from Thomas Baker company and sodium chloride (NaCl) powder with 99.9% purity by weight were used as supporting electrolytes. Anhydrous ferric chloride ($FeCl_3$) powder with 98% purity by weight, from the Alpha Chemike company and anhydrous aluminum chloride ($AlCl_3$) powder with 98% purity by weight, from the Central Drug House Ltd. company, were used as metal sources for the metal impregnation process. A 1M solution of hydrochloric acid (HCl, 37%, liquid, Sigma-Aldrich) and sodium hydroxide (NaOH, 97%, pellets, Sigma-Aldrich) was prepared to alter the original pH of the treated effluent.

TABLE II.   PHYSICAL PROPERTIES OF THE COMMERCIAL GAC

Parameters	Values
Test standard	ASTM-D
BET surface area (m^2/g)	950-1200
Iodine Number (mg/g)	900-1150
Total ash content	Max. 5%
Hardness	Min. 97%
Apparent density (Kg/m^3)	460±40
Moisture content	8% (as packed)
Attrition	Max. 3%
Particle size	8×30 mesh available

B. Preparation of the Metal-Impregnated Granular Activated Carbon (MIGAC)

After being sieved to a particle size of over 1mm in diameter, commercial GAC particles with a particle size of (8×30) mesh were washed with deionized distilled water to remove impurity compounds. Finally, the particles were dried

in an oven at 105°C for 24h. Subsequently, the GAC was impregnated with molar ratios 1:10 as Al: AC, 1:10 as Fe: AC, 1:1:10 as Al:Fe:AC, 1:2:10 as Al:Fe:AC, and 2:1:10 as Al:Fe:AC using $AlCl_3$ and $FeCl_3$ as the Al and Fe sources respectively. It was then mixed with 50ml deionized water at 90°C for 4h. The resulting solution was mixed in a 500ml round–bottom flask with two necks: one neck was fitted with water–cooling reflux condenser and the other was equipped with a thermometer to measure the temperature. The reaction was carried out at atmospheric pressure. Agitation and heating of the flask were done by oil bath (engine oil from Al-Daura refinery with flash point 220°C) on a magnetic stirrer hot plate. Heidolph™ 505-20000-00, 0-300°C, 0-1400rpm was utilized for obtaining homogeneous solution at a rotation speed of 200rpm, where the temperature of the mixture in the heated flask was kept constant by using voltage regulator (Single – phase AC voltage regulator, 220V regulator adjustable 0-300V, max power 500W) to control the heat of the heater. After another wash with deionized distilled water, the MIGAC was dried in a 105°C oven for 24h.

C. Experimental Procedure

A preliminary feasibility test was conducted to determine the suitability of the TEC-MIGAC system for COD and turbidity elimination from the refinery effluent. This performance was compared to those of other systems, including an adsorption and Conventional EC (CEC) system and a raw granular activated carbon with CEC system (TEC-RGAC). All batch studies were conducted under the same experimental conditions: 1.0L working volume, duration of 120min, 10g raw activated carbon or MIGAC, pH=7, and 30V applied voltage. The experiments were conducted by using the laboratory setup shown in Figure 1. The tubular electrochemical reactor (Figure 1(a)) was made from Perspex glass with 30mm diameter and 140mm height. The wastewater was pumped to the cylindrical EC cell using a peristaltic pump (RUNZE, single stage pump, made in China) with a maximum flow rate of 200mL/min. The aluminum and stainless steel disk electrodes (30mm in diameter and 5mm in thickness) were pierced with 1mm holes and were connected to a DC power source. Each electrode had total effective surface area of $7.065cm^2$. The distance between the electrodes did not alter and was kept at 6cm despite the rapid electron transfer rate between the anode and the cathode that was caused by the particle electrodes [38]. The aluminum anode was positioned below the cathode, and water was circulated in the direction from the anode to cathode. In the case of 3D reactor, a packed bed of GAC or MIGACs was placed between the anode and the cathode. During each experiment, for the purpose of delivering an adequate voltage, a digital direct current power supply of the type (UNI-T, UTP3315PF) that ranged from 0-30V and 0-5A was used. A multimeter was used to measure the system's current and voltage. The effluent from the EC unit was sent to a settling tank, where the overflow was pumped back to the EC cell. To remove the electrodes' oxide and passivation layers, they were washed in HCl solution (35%) and acetone [39]. HCl solution (0.1N) and NaOH solution (0.1N) were used to adjust pH. NaCl and Na_2SO_4 were used as electrolytes. NaCl solution was utilized as an extra electrolyte because it has a lot of benefits, including the ability of chloride ions to considerably lessen the

negative effect of other anions such HCO_3^- and SO_4^{2-}. The carbonate ion would cause the precipitation of Ca^{2+} or Mg^{2+} ions, which create an insulating layer on the electrode surface. This insulating layer would significantly lower the electrochemical cell's current efficiency and treatment conversion while substantially raising its ohmic resistance. As a result, it is proposed that among the current anions, 20% Cl^- be present to enable normal EC activity in water treatment [40]. The ambient temperature for all tests was 25 ±2°C. After the experiment, the samples were filtered using filter papers with size 150mm before being analyzed. TDS, pH, turbidity, and the initial and final COD concentrations were also measured.
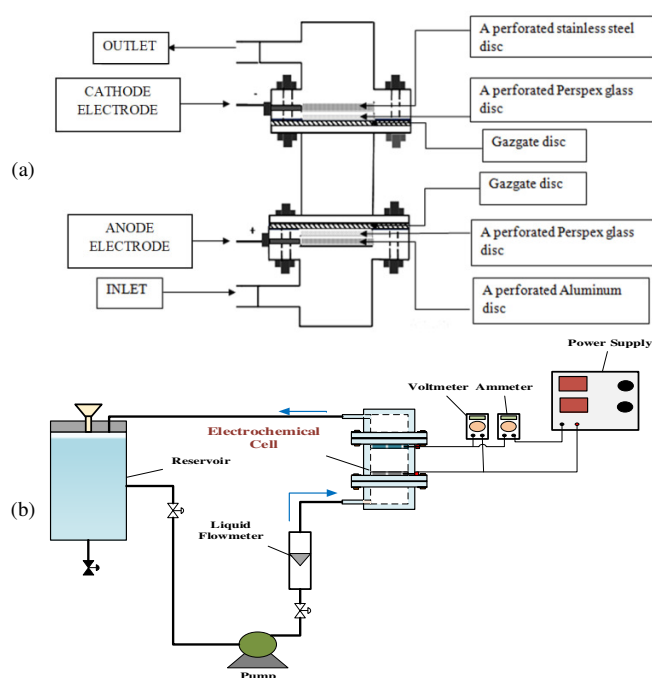
Fig. 1.   Schematic diagram of (a) the EC cell, (b) the EC system.

D. Methods of Analysis

Using Spectro Xepos XRF (Ametek Co., Germany), the textural qualities of raw granular and MIGAC were evaluated. The morphology and microstructure were examined with SEM. At the same surface locations as the SEM, EDS was also used to undertake surface element analysis concurrently (INSPECT, F50, REI Co., Netherland). Physical properties, BET specific surface area, and total pore volume were determined using the SA-9600 model (Horibe USA brand) using nitrogen gas as adsorbate. Lovibond COD VARIO photometric detector (COD Setup, MD 200, UK) was used for COD analysis. For the COD test, a sample of 2ml of the substrate was completely thermally oxidized using a standard oxidation reagent in a cuvette tube. The combination of the substrate sample and the standard oxidation reagent was heated at 150°C for 2h to guarantee that the substrate had completely oxidized. The concentration of the COD of the organics was determined in mg/L by a COD photometer in a thermo-reactor (RD 125, Lovibond, Germany). Turbidity was measured with a compact Lovibond® infrared turbidity meter Turbi Check. The turbidity and COD removal

efficiency were evaluated based on (1), where Ci is the initial and Cf the final concentration (mg L^{-1}) [41]:

$$RE\% = \frac{ci - cf}{ci} \times 100 \quad (1)$$

The quantity of electrical energy that is used up throughout the EC process in order to eliminate 1kg of COD is referred to as the Energy Consumption (*EC*). *EC* may be determined in terms of kWh/kg by [42]:

$$EC = \frac{U.I.t \times 1000}{(CODi - CODf)V} \quad (2)$$

where COD_i and COD_f are the initial and final chemical oxygen demand (mg/L), U is the applied cell voltage (V), I is the current (A), t is the electrolysis time (h), and V is the effluent volume (L). A TDS-meter (161002 PurePro Inc.) was used to test the TDS, and a pH-meter (HANNA Instruments Co.) was used to determine the pH. Electrical conductivity was measured with a HANNA HI-99301 meter.

III. RESULTS AND DISCUSSION

A. Textural Properties

Table III shows the physical properties of unprocessed GAC and MIGACs, based on nitrogen adsorption and desorption isotherms, specific surface area, and total pore volume. It is evident that following ferric-aluminum impregnation, MIGACs' specific surface area and total pore volume both significantly reduced to 893.7, 878, 874, 840, and 797.5m^2/g and 0.21702, 0.20075, 0.19502, 0.19722, 0.18388, and 0.01376m^3/g for MIGAC(Fe), MIGAC(Al), MIGAC(1:1),

MIGAC(1:2), and MIGAC(2:1) respectively. These decreased physical characteristic values point to a preferential distribution of metal oxides in the pore mouth. Certain micropores were subsequently obstructed, along with the development of meso- or macro-porous structures and the covering of binders to the active sites created by ferric or aluminum oxides [43, 44].

The evidence for this may also be seen rather obviously in the micro structural analysis. Images from a scanning electron microscope of RGAC (A1-4), MIGAC(Fe) (B1-4), MIGAC(Al) (C1-4), MIGAC(1:1) (D1-4), MIGAC(1:2) (E1-4), and MIGAC(2:1) (F1-4) are presented in Figure 2. While the raw GAC's porous nature is easily seen in Figure 2 (A1-4), it was observed that some porous structural collapse took place when the raw GAC was impregnated with metal, leading to clogs, as shown in Figure 2 (A1-3), (B1-3), (C1-3), (D1-3), (E1-3), and (F1-3). Also, in Figure 2, A4 can be seen showing the surface of raw GAC before impregnation and Figure 2 B4, C4, D4, E4, and F4 emphasize that the metal oxide aggregates formed on the surface of raw GAC after the wet impregnation have a spherical shape. It was calculated that the average crystallite size of metal oxides was in the range of (21.24-32.58), (21.32-27.38), (26.23-62.77), (55.67-76.49), (18.75-26.89) nm for MIGAC(Fe), MIGAC(Al), MIGAC(1:1), MIGAC(1:2), and MIGAC (2:1) respectively. From the image in Figure 2 F4, it can be seen that iron and aluminum oxides were aggregated homogenously on the surface of the raw GAC and the range of the size of the metal oxides was smaller than the ranges of the other GAMIs.

TABLE III.   RAW GAC AND MIGAC MICROSTRUCTURES

Properties	RGAC	MIGAC (Fe)	MIGAC (Al)	MIGAC (1:1)	MIGAC (1:2)	MIGAC (2:1)
BET specific surface area (m^2/g)	1086	893.7	878.7	874	840	797.5
Total pore volume (cm^3/g)	0.21702	0.20075	0.19502	0.19722	0.18388	0.01376

TABLE IV.   EDS ELEMENTAL COMPOSITION OF RAW GAC AND MIGACs

Element	RGAC		MIGAC(Fe)		MIGAC(Al)		MIGAC(1:1)		MIGAC(1:2)		MIGAC(2:1)	
	Weight %	Atomic %	Weight %	Atomic %	Weight %	Atomic %	Weight %	Atomic %	Weight %	Atomic %	Weight %	Atomic %
C	88.82	92.7	83.17	88.7	85.1	89.9	78.91	87.66	80.6	88.5	73.95	83.6
O	7.28	5.7	12.13	9.7	10.7	8.5	9.5	7.9	10	8.3	13.33	11.3
Fe	-	-	1.63	0.4	-	-	1.99	0.51	3.2	0.78	1.65	0.43
Al	0.207	0.1	0.203	0.1	1.3	0.6	1.034	0.53	0.8	0.42	1.67	0.87
Si	1.78	0.8	0.22	0.1	0.1	0.1	0.42	0.2	0.7	0.3	0.21	0.1
Cl	-	-	2.66	1	2.6	0.9	8.16	3.2	4.7	1.7	9.02	3.6
Ca	-	-	-	-	-	-	-	-	-	-	-	-
K	1.51	0.5	-	-	-	-	-	-	-	-	-	-
Mg	0.38	0.2	-	-	-	-	-	-	-	-	0.18	0.1
Total	100	100	100	100	100	100	100	100	100	100	100	100

At the same surface areas where the SEM was used, an element analysis of the surface was also conducted at the same time as the EDS. Table IV displays the weight and atomic percentages of the raw and MIGAC elements. It can be seen that the level of Al changed to 0.6%, 0.53%, 0.42%, and 0.87% for MIGAC(Al), MIGAC(1:1), MIGAC(1:2), and MIGAC(2:1) respectively, and the level of Fe changed to 0.4%, 0.51%, 0.78%, and 0.43% for MIGAC(Fe), MIGAC(1:1), MIGAC(1:2), and MIGAC(2:1) respectively. Aluminum and ferric iron were completely impregnated into raw GAC, as determined by the atomic percentage following impregnation.

Clearly, AlCl$_3$ and FeCl$_3$ were the source of the Cl after impregnation. Aluminum and ferric iron were likely bonded to MIGAC in the form of aluminum oxide and iron oxide, given the increased oxygen concentration in MIGAC compared to the raw GAC.

XRF chemistry analysis was used to confirm the oxide form of the metals in both raw GAC and MIGAC. Formation of oxides by metals on each other's surfaces is documented in Table V, which shows that aluminum oxide and ferric oxide are the most common forms of these metals.

TABLE V.   XRF ANALYSIS WAS USED TO DETERMINE THE METAL OXIDE FORM IN RAW GAC AND MIGAC

Components	RGAC (mass%)	MIGAC(Fe) (mass%)	MIGAC(Al) (mass%)	MIGAC(1:1) (mass%)	MIGAC(1:2) (mass%)	MIGAC(2:1) (mass%)
MgO	0.4573	1.148	0.505	0.741	1.200	0.817
Al_2O_3	0.2899	0.2153	0.9091	2.0521	1.9941	3.3345
SiO_2	1.039	0.8847	0.3724	0.1434	0.1846	0.1765
P_2O_5	0.3564	0.1924	0.2151	0.1826	0.1376	0.1732
SO_3	0.09675	0.09694	0.04981	0.02413	0.02272	0.03716
Cl	0.05731	1.751	1.610	2.892	4.081	4.2253
K_2O	2.096	0.0645	0.0645	0.0646	0.1045	0.0666
CaO	2.919	1.346	1.619	1.031	1.579	1.239
TiO_2	0.00307	0.00317	< 0.0013	0.00344	0.00281	0.00466
V_2O_5	< 0.0011	< 0.00072	< 0.0013	< 0.0011	< 0.00068	< 0.00069
Cr_2O_3	< 0.00022	< 0.00015	0.00099	0.00109	0.00050	0.00099
MnO	0.00183	0.00046	0.00056	0.00203	0.00206	0.00326
Fe_2O_3	0.03133	1.677	0.04100	1.962	3.428	1.7841
CoO	< 0.00039	< 0.00039	< 0.00039	< 0.00039	< 0.00039	< 0.00039
NiO	0.00081	0.00064	0.00118	0.00122	0.00085	0.00086
CuO	0.00318	0.00566	0.00366	0.00618	0.00627	0.00678
ZnO	0.00062	0.3631	0.00126	0.00199	0.00141	0.00162
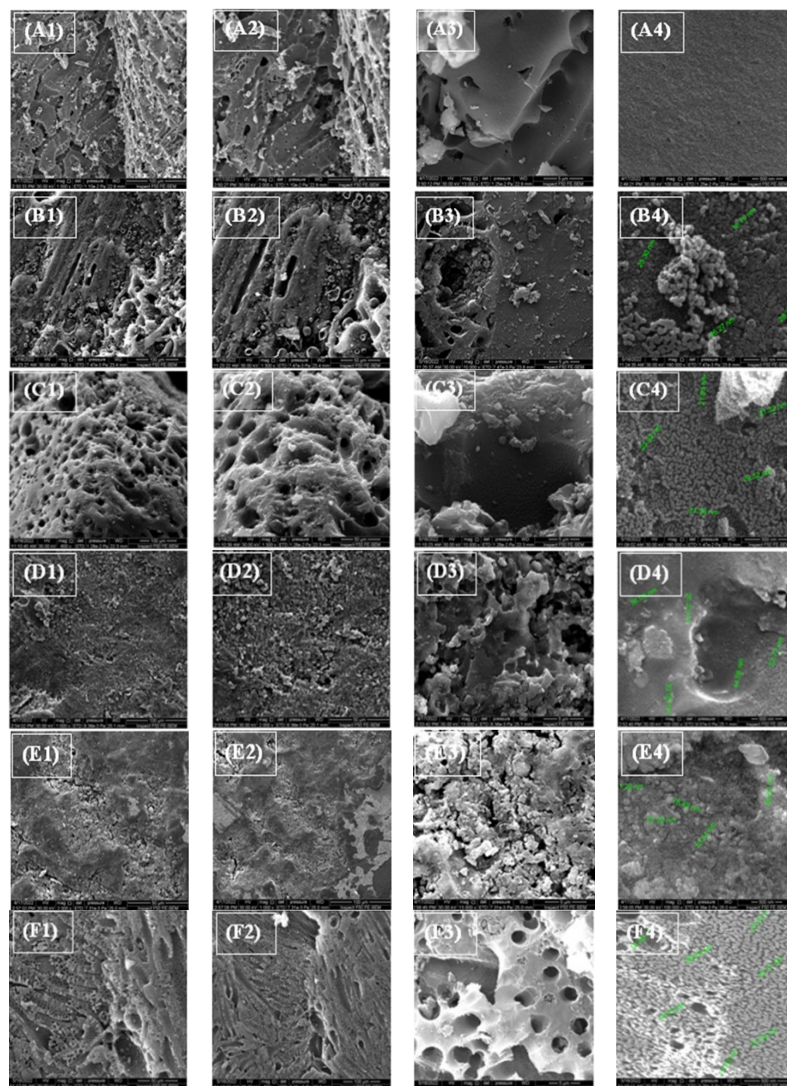
Fig. 2.   SEM images of (A1-4) RGAC, (B1-4) MIGAC(Fe), (C1-4) MIGAC(Al), (D1-4) MIGAC(1:1), (E1-4), MIGAC(1:2), and (F1-4), MIGAC(2:1) at different expansion ratios.

B. Influence of Auxiliary Electrolyte Dosing

The solution's conductivity is essential for increasing process effectiveness and lowering current density. The lower potential flowing in the circuit during treatment is maintained via conductivity, which also results in less electricity being used. The conductivity of the effluent caused the heterogeneous ions to transfer in the EC method. Electrolytes Na_2SO_4 and NaCl were employed in this treatment [41]. Additionally, SO_4^{-2} ions do not corrode as much as the chloride species. The great corrosive capability of Cl^- ions aids in the disintegration of the coagulant. The needed voltage will be significantly lower in the presence of chloride ions than it would be in the presence of SO_4^{-2} ions. Comparing the adsorption behaviors of Cl^- and SO_4^{-2} ions on the Al electrode, it has been discovered that Cl^- had a lower degree of adsorption than SO_4^{-2} [45]. Chloride ions are transformed into active chlorine species when the current density is sufficiently high. These species then participate in the oxidation of ferrous ions and organic materials [46].

Table VI and Figure 3 show the effect of variable concentrations of electrolytes on the removal of chemical oxygen demand. EC process was performed using applied voltage of 30V, time 120min, pH 7, and 10g raw activated carbon. As shown in Table VI, when the wastewater treated without any added electrolyte concentration of Na_2SO_4 or NaCl, the conductivity and applied current were 2.66mS/cm and 15.1mA respectively and the COD removal was 58.8% at 20min, whereas it increased to 72.3% at 120min. The synergistic effects of raw GAC adsorption in the GAC-three dimensional EC system may be responsible for these results. After adding the electrolytes (2.5g NaCl, 3.5g Na_2SO_4, 2.5g NaCl + 3.5g Na_2SO_4, and 2.5g NaCl + 7g Na_2SO_4), the conductivity and the applied current were 7, 7.44, 12.16, and 20mS/cm and 45, 56, 87, and 98mA respectively. As shown in Figure 4, the COD removal rate was improved when a mixture of electrolytes (NaCl + Na_2SO_4) was added to the reaction system at different concentrations. Increment in removal efficiency was observed from 90.7% to 93.7% after 120min for 2.5g NaCl + 3.5g Na_2SO_4. This might be attributed to the fast flow of electrolyte ions. Additionally, no additional improvement in removal efficiency was observed when the supporting electrolyte concentration of Na_2SO_4 was raised to 7g/L, which may be caused by an expansion of the passivation layer. Therefore, 2.5g Nacl and 3.5g Na_2SO_4 were selected as the optimum electrolyte concentration and this is in agreement with the findings of the authors in [37], which used NaCl with a concentration of 4g/L to obtain 13.6mS/cm conductivity for removing carbamazepine by a three-dimensional electrochemical process utilizing particle electrodes made of carbon-based adsorbent material.

C. Feasibility Test

To find out whether the TEC-MIGAC system is appropriate for removing COD and turbidity from refinery effluents, a feasibility test was carried out. An adsorption system, a CEC system, and a Raw GAC with CEC (TEC-RGAC) system were used and their performance was compared. Because of its great adsorption capability, GAC adsorption is a well-established technology used in wastewater post-treatment and water

purification. The adsorption processes took place in the same cell without supplying an electric field.

Electrolyte concentration (g/L)	Initial conductivity (µS/cm)	Current (mA)	COD removal (%)		SEC (kWh/kg COD)
			20min	120min	
Without salt	2660	15.1	58.8	72.3	0.80
2.5g NaCl	7000	45	73.6	84.6	1.64
3.5g Na_2SO_4	7440	56	75.1	85.2	2.61
2.5g NaCl + 3.5g Na_2SO_4	12160	87	90.7	93.7	3.68
2.5g NaCl + 7g Na_2SO_4	20000	98	91.7	95.4	4.68
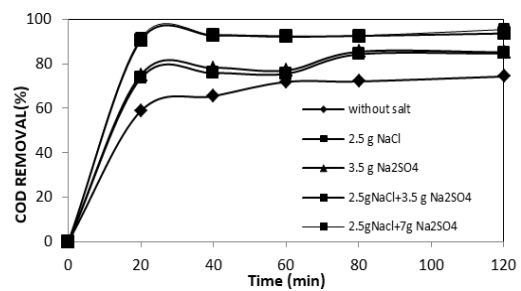
Fig. 3.   Electrolyte dose effect on COD removal (30V, 120min, pH=7, and 10g raw activated carbon).
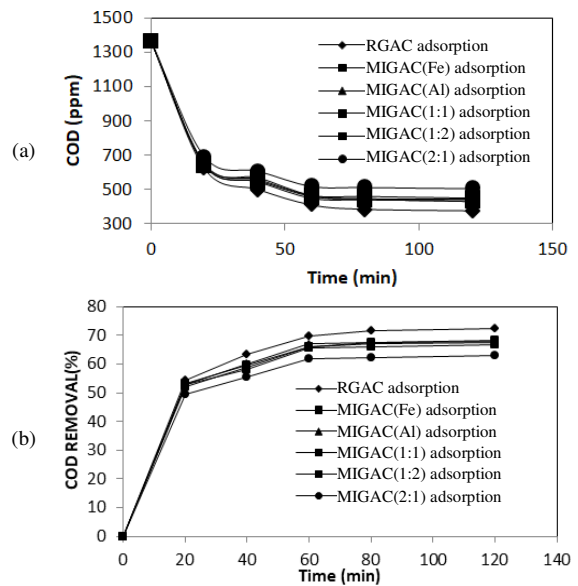
Fig. 4.   (a) COD profile with time, (b) COD removal of the adsorption process on different impregnated activated carbon (1361mg/L initial COD, 10g of AC or MIGAC dosage, and 175mL/min flow rate).

In Batch test I, similar experimental settings were used for each experiment in the adsorption procedure (120min, 10g of AC or MIGAC dosage, and 175ml/min flow rate). In Figures 4-5 and Table VII, it can be seen that the raw GAC system's adsorption system achieved maximum COD removal. In the adsorption system by raw GAC, the COD and turbidity decreased quickly to 619mg/L and 2.48NTU respectively in the first 20min, and then slowly to 376mg/L and 2.31NTU at

120min, while 72.3% COD removal and 98.9% turbidity were obtained at the 120min treatment. COD and turbidity were reduced to 638, 640, 649, 643, and 689mg/L and 13.4, 1.94, 1.89, 32.1, and 11NTU respectively in the first 20min, and then continuously to 430, 435, 444, 450, and 505mg/L and 1.165, 2.02, 8.9, 5.98, and 10NTU at 120min for MIGAC(Fe), MIGAC(Al), MIGAC(1:1), MIGAC(1:2), and MIGAC(2:1), respectively corresponding to 68.41, 68.03, 67.38, 66.94, and 62.89% of COD removal at 120min. The high COD removal of raw GAC compared to the MIGAC systems may be due to the fact that metal oxides are preferentially dispersed in the pore mouth, blocking some micropores and constructing a mesoporous or macroporous structure, and overlaying binders to the activated sites created by ferric or aluminum oxides. This is in agreement with the results of [38]. A significant improving in TDS removal was observed for impregnated activated carbons with highest removal by MIGAC (2:1) as shown in Table VII.
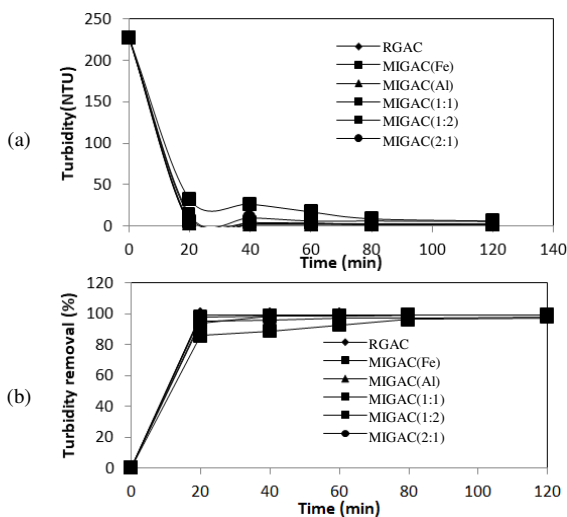
Fig. 5.   (a) Turbidity profile with time, (b) turbidity removal for adsorption process on the different impregnated activated carbon methods (227NTU initial turbidity, 10g of AC or MIGAC dosage, and 175mL/min flow rate).

TABLE VII.   COD AND TURBIDITY REMOVAL

Type of adsorbent	COD removal %		Turbidity removal %		TDS removal %	
	20 min	120 min	20 min	120 min	20 min	120 min
GAC	54.5	72.3	98.9	98.9	0	2.89
MIGAC(Fe)	53.1	69.7	94.09	99.2	5.79	25.60
MIGAC(Al)	52.3	69.06	98.9	99.15	14.05	17.87
MIGAC(1:1)*	52.9	70.24	97.6	99.16	10.14	12.07
MIGAC(1:2)*	52.7	68.55	85.8	97.36	15.94	30.43
MIGAC(2:1)*	49.3	66.78	95.15	97.53	50.72	52.17

In batch test II, removing turbidity and COD from real refinery wastewater was considered and comparisons were made between the CEC system with aluminum and stainless steel electrodes, TEC-RGAC, and TEC-MIGAC systems. Table VIII and Figures 6 and 7 demonstrate the performance of RGAC and MIGACs in removing turbidity and COD at an initial pH of 7 and a reaction duration of 120min, using 30V applied voltage, 10g RGAC or MIGAC, and 2.5g/L NaCl + 3.5

g/L Na_2SO_4 as supporting electrolyte. In the past, stainless steel and aluminum electrodes have been widely employed in electrochemical wastewater treatment systems due to their availability and low cost. With chloride in the solution, the primary direct electrochemical reaction may occur and is heavily dependent on it. Hypochlorous acid/hypochlorite ions ($HOCl/OCl^-$), which are powerful oxidants, can be generated in the solution during the direct electrochemical reaction due to the anode and cathode ionization processes, and as a result, turbidity and COD will be reduced [47-49].

In CEC, as shown in Figures 6 and 7, COD and turbidity decreased to 450mg/L and 2.11NTU respectively, in the first 20min, then to 200mg/L and 2.06NTU in the following 100min. After 120min of treatment, 85.3% of COD and 99.04% turbidity removals were achieved.
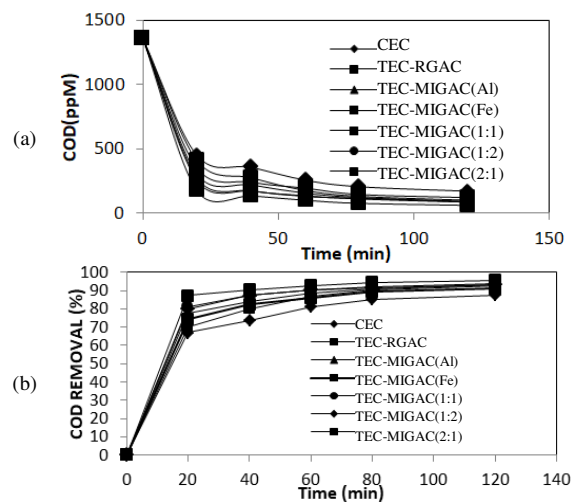
Fig. 6.   (a) COD profile with time and (b) COD removal for performance comparison between CEC system with aluminum and stainless steel electrodes, TEC-RGAC, and TEC-MIGAC systems (1361mg/L initial COD, 7 pH, 30V, 10g of RGAC or MIGAC dosage, 175mL/min flow rate and 2.5g/L NaCl + 3.5g/L Na_2SO_4 as supporting electrolyte).

As the next step, we improved and compared the removal performance of the traditional EC system by introducing TEC-RGAC and TEC-MIGACs particles. Metal ions (aluminum and ferric iron) produced from MIGACs during the EC were predicted to have a greater influence on removal efficiency. The contrary of what was anticipated happened when RGAC and MIGACs were added to the reactor and comparable efficacy was seen in both systems. After 20min response time, the turbidity and COD were promptly gone, whereas the COD removal could be attributed to the precipitation of dissolved organics. The amount of hydroxide flocs, which was associated with EC time and cell current, evaluated the effectiveness of COD removal. Longer observation times and greater cell current levels indicated higher COD elimination efficiency [50]. After 120min response time, turbidity and COD removal were 99.14% and 92.65% in the TEC-RGAC system, and 99.36, 98.97, 99.41, 99.4, and 99.43% and 91.18, 93.46, 93.75, 93.39, and 95.74% in the TEC-MIGAC systems. These results may have been brought about by the additive effect of raw GAC adsorption in the TEC-RGAC system, which has more

distinguishable textural properties than MIGAC, including BET surface area, total pore volume, and micropore structure. Traditional two-dimensional electrode systems have a low COD removal effectiveness (76.12% after 60min). By using a three-dimensional electrocoagulation reactor system, COD removal efficiency increased significantly to 87.06, 88.61, 85.75, 90.08, 90.44, and 92.65% after 60min. Also, it was found that the MIGAC with a 2:1 molar ratio of aluminum to ferric metal ions had the highest COD removal. Results showed that MIGAC could show substantially higher removal efficiency than the GAC addition due to the impact of metal (aluminum and iron) ions created by the addition on EC.
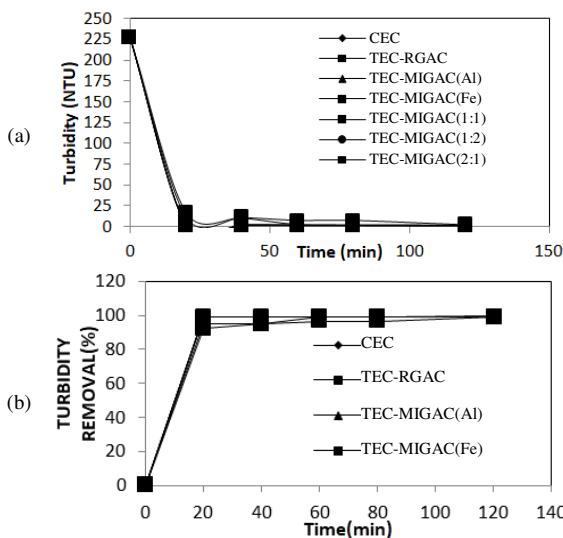
Fig. 7. (a) Turbidity profile with time and (b) Turbidity removal for performance comparison between CEC system with aluminum and stainless steel electrodes,TEC-RGAC, and TEC-MIGAC systems (227NTU initial turbidity, 7 pH, 30V, 10g of RGAC or MIGAC dosage, 175mL/min flow rate and 2.5g/L NaCl + 3.5g/L Na$_2$SO$_4$, as supporting electrolyte.

TABLE VIII. COD AND TURBIDITY REMOVAL OF CRC, TEC-GAC, AND TEC-MIGAC SYSTEMS

Type of particle electrode	COD removal %		Turbidity removal %		TDS removal %		Energy consumption (kWh/kg COD)
	20 min	120 min	20 min	120 min	20 min	120 min	
CEC	66.93	85.3	99.04	99.25	46.23	50.75	12.777
TEC-GAC	69.88	92.65	98.87	99.14	46.23	49.84	3.697
TEC-MIGAC(Fe)	74.14	91.18	99.22	99.36	45.93	53.16	3.735
TEC-MIGAC(Al)	77.59	93.46	94.88	98.97	42.77	50.3	3.768
TEC-MIGAC (1:1)	81.26	93.75	92.42	99.41	48.49	52.56	3.602
TEC-MIGAC (1:2)	79.87	93.39	98.84	99.4	48.34	52.25	3.676
TEC-MIGAC (2:1)	87.14	95.74	99.20	99.43	51.35	55.57	3.920

The fundamental issue of the GAC adsorption technique is that the porosity eventually gets saturated and inefficient, rendering the technique worthless [51]. As a consequence, it could be challenging to measure and evaluate GAC's function as a particle electrode or adsorbent if raw GAC is utilized

directly as a particle electrode in a three-dimensional EC reactor system. In this respect, another test was conducted, and the reaction time for each set was lowered to 80min, since the removal efficiency increased marginally with increasing reaction time. As shown in Figure 8, increasing the repetition cycle was associated with a decrease in COD removal efficiency in the TEC-RGAC system. However, those efficiencies were kept constant approximately in the TEC-MIGAC (2:1) system. After 10 repetitions, the apparent value of the TEC-MIGAC (2:1) system was greater than that of the TEC-RGAC system, with the TEC-MIGAC (2:1) system achieving 90.22% COD removal, while the TEC-RGAC system achieved 63.72%. Metal ions (iron/aluminum) were first dissolved during the anode reaction step of the electrocoagulation process. Instantaneously upon reaching a certain pH, they hydrolyzed to generate polymeric iron and aluminum oxyhydroxides (Fe(OH)$_3$ and Al(OH)$_3$) respectively, which are effective coagulating agents [52].
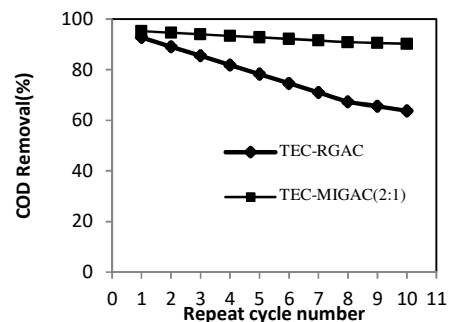
Fig. 8. Repeated test between the GAC and the TEC-MIGAC system.

D. Comparison with Previous Studies

Authors in [20] utilized an electrochemical technique with a three-dimensional multi-phase electrode. Fe particulates and air were injected into a conventional two-dimensional reactor to remediate effluents from a petroleum refinery. The initial pH and cell voltage, as well as the effect of Fe particles and air have on the electrochemical process, were both subjects of the research that was carried out as a part of the process of determining the optimal experimental settings. The results of their investigation found that the effluent had a COD removal effectiveness that was good (92.8%). Authors in [53] treated wastewater from a local petroleum refinery using an aluminum electrode and having two distinct COD levels in a continuous electrochemical cell. They investigated the impacts of inflow flow rate, initial pH, and current density. They demonstrated that EC may reduce COD by up to 57% when used under ideal circumstances. Authors in [54] treated effluents from a heavy oil refinery using a Three-Dimensional Electrode Reactor (TDER) equipped with a combination particle electrode consisting of GAC and Porous Ceramsite Particle (PCP) and an anode of the DSA type. When comparing the TDER to the two-dimensional electrode reactor, it was discovered that it was more effective at removing COD and that the combination particle electrode was advantageous in increasing the COD removal efficiency and decreasing energy consumption. Under the best experimental conditions (GAC percentage = 75%,

current density = 30mA/cm^2, not altered pH, and treatment time = 100min), the maximum removal of COD, total organic carbon, and toxicity units from the treated effluent were 45.5%, 43.3%, and 67.25% respectively. It was found that the metal impregnated granular activated carbon with a 2:1 molar ratio of aluminum to ferric metal ions had higher COD removal in comparison with that obtained from [38], which used metal impregnated activated carbon (Al:Fe) with a molar ratio of (1:1) as a moving particle EC electrode in a three-dimensional EC process to treat wastewater from real cotton textiles with a COD content of 685mg/L. COD removal after treatment was 81.6% after 120min of reaction time, 10g MIGAC, and 30V applied voltage at pH=7.7. Therefore, the present system exhibited excellent results in terms of COD and turbidity removal using the new design of the three dimensional electrode.

IV. CONCLUSIONS

In this study, the treatment of refinery wastewater using a new three – dimensional electrocoagulation approach was proposed and investigated. The new cell utilizes Granular Activated Carbon (GAC) and Metal-Impregnated GAC (MIGAC) as third particle electrodes. The three-dimensional electrocoagulation reactor system is an interesting technology for improving refinery wastewater treatment in electrocoagulation, according to a feasibility test employing a typical two-dimensional electrode, adsorption process, and the three-dimensional electrocoagulation system ,where the COD removal efficiency for the adsorption process was 72.37, 68.41, 68.04, 67.38, 66.94, and 62.84% after 120min for Raw GAC (RGAC), MIGAC(Fe), MIGAC(Al), MIGAC(1:1), MIGAC(1:2), and MIGAC(2:1) respectively while 85.3% was in the conventional two dimensional electrode system after 120min.

The COD removal efficiency was enhanced by using the three-dimensional electrocoagulation method, reaching 92.65, 93.46, 91.18, 93.75, 93.39, and 95.74% after 120min for TEC-RGAC, TEC-MIGAC(Al), TEC-MIGAC(Fe), TEC-MIGAC(1:1), TEC-MIGAC(1:2), and TEC-MIGAC(2:1), respectively based on the operating conditions of: 1361 initial COD, 7 pH, 30V, 10g of AC or MIGAC dosage for the three dimensional system, 175mL/min flow rate and 2.5g/L NaCl + 3.5g/L Na$_2$SO$_4$ as supporting electrolytes.

The results showed that the MIGAC addition exhibits considerably larger removal efficiency than the RGAC addition because of the influence of metal ions created by the MIGAC on the electrocoagulation. Besides, it was found that the MIGAC with a molar ratio of aluminum to ferric metal ion (2:1) had higher COD removal in comparison with previous studies. Also, in the present study, the energy consumption was reduced from 12.78KWh/Kg COD for the conventional two dimensional system to 3.9KWh/Kg COD when using the three dimensional TEC-MIGAC (2:1). Considering the obtained results, the 3D process allowed efficient removal of COD after a shorter period when compared with the 2D process and also decreased energy consumption.

REFERENCES

[1] H. Wake, "Oil refineries: a review of their ecological impacts on the aquatic environment," *Estuarine, Coastal and Shelf Science*, vol. 62, no. 1, pp. 131–140, Jan. 2005, https://doi.org/10.1016/j.ecss.2004.08.013.

[2] M. A. Tony, P. J. Purcell, and Y. Zhao, "Oil refinery wastewater treatment using physicochemical, Fenton and Photo-Fenton oxidation processes," *Journal of Environmental Science and Health, Part A*, vol. 47, no. 3, pp. 435–440, Feb. 2012, https://doi.org/10.1080/10934529.2012.646136.

[3] J. Saien and H. Nejati, "Enhanced photocatalytic degradation of pollutants in petroleum refinery wastewater under mild conditions," *Journal of Hazardous Materials*, vol. 148, no. 1, pp. 491–495, Sep. 2007, https://doi.org/10.1016/j.jhazmat.2007.03.001.

[4] M. Yalda, M. M. A. Torabi, and A. Fouladitajar, "Refinery and petrochemical wastewater treatment," in *Sustainable Water and Wastewater Processing*, Amsterdam, Netherlands: Elsevier, 2019, pp. 55–91.

[5] A. N. Laghari, Z. A. Siyal, D. K. Bangwar, M. A. Soomro, G. D. Walasai, and F. A. Shaikh, "Groundwater Quality Analysis for Human Consumption: A Case Study of Sukkur City, Pakistan," *Engineering, Technology & Applied Science Research*, vol. 8, no. 1, pp. 2616–2620, Feb. 2018, https://doi.org/10.48084/etasr.1768.

[6] A. A. Mahessar, A. L. Qureshi, A. N. Laghari, S. Qureshi, S. F. Shah, and F. A. Shaikh, "Impact of Hairdin, Miro Khan and Shahdad Kot Drainage on Hamal Dhand, Sindh," *Engineering, Technology & Applied Science Research*, vol. 8, no. 6, pp. 3652–3656, Dec. 2018, https://doi.org/10.48084/etasr.2389.

[7] A. N. Laghari, Z. A. Siyal, M. A. Soomro, D. K. Bangwar, A. J. Khokhar, and H. L. Soni, "Quality Analysis of Urea Plant Wastewater and its Impact on Surface Water Bodies," *Engineering, Technology & Applied Science Research*, vol. 8, no. 2, pp. 2699–2703, Apr. 2018, https://doi.org/10.48084/etasr.1767.

[8] P. A. Pugazhendi, H. Abbad Wazin, H. Qari, J. M. A.-B. Basahi, J. J. Godon, and J. Dhavamani, "Biodegradation of low and high molecular weight hydrocarbons in petroleum refinery wastewater by a thermophilic bacterial consortium," *Environmental Technology*, vol. 38, no. 19, pp. 2381–2391, Oct. 2017, https://doi.org/10.1080/09593330.2016.1262460.

[9] N. M. Makkiya and I. A. W. Al-Baldawi, "Biodegradation of Total Petroleum Hydrocarbon from Al-Daura Refinery Wastewater by Rhizobacteria," *Journal of Engineering*, vol. 26, no. 1, pp. 14–23, 2020, https://doi.org/10.31026/j.eng.2020.01.02.

[10] S. Arefi-Oskoui, A. Khataee, M. Safarpour, and V. Vatanpour, "Modification of polyethersulfone ultrafiltration membrane using ultrasonic-assisted functionalized MoS2 for treatment of oil refinery wastewater," *Separation and Purification Technology*, vol. 238, May 2020, Art. no. 116495, https://doi.org/10.1016/j.seppur.2019.116495.

[11] I. Ulhaq, W. Ahmad, I. Ahmad, M. Yaseen, and M. Ilyas, "Engineering TiO2 supported CTAB modified bentonite for treatment of refinery wastewater through simultaneous photocatalytic oxidation and adsorption," *Journal of Water Process Engineering*, vol. 43, Oct. 2021, Art. no. 102239, https://doi.org/10.1016/j.jwpe.2021.102239.

[12] B. Singh and P. Kumar, "Pre-treatment of petroleum refinery wastewater by coagulation and flocculation using mixed coagulant: Optimization of process parameters using response surface methodology (RSM)," *Journal of Water Process Engineering*, vol. 36, Aug. 2020, Art. no. 101317, https://doi.org/10.1016/j.jwpe.2020.101317.

[13] S. H. Ammar, N. N. Ismail, A. D. Ali, and W. M. Abbas, "Electrocoagulation technique for refinery wastewater treatment in an internal loop split-plate airlift reactor," *Journal of Environmental Chemical Engineering*, vol. 7, no. 6, Dec. 2019, Art. no. 103489, https://doi.org/10.1016/j.jece.2019.103489.

[14] R. N. Abbas and A. S. Abbas, "The Taguchi Approach in Studying and Optimizing the Electro-Fenton Oxidation to Reduce Organic Contaminants in Refinery Wastewater Using Novel Electrodes," *Engineering, Technology & Applied Science Research*, vol. 12, no. 4, pp. 8928–8935, Aug. 2022, https://doi.org/10.48084/etasr.5091.

[15] H. M. Ibrahim and R. H. Salman, "Study the Optimization of Petroleum Refinery Wastewater Treatment by Successive Electrocoagulation and Electro-oxidation Systems," *Iraqi Journal of Chemical and Petroleum Engineering*, vol. 23, no. 1, pp. 31–41, Mar. 2022, https://doi.org/10.31699/IJCPE.2022.1.5.

[16] S. S. Alkurdi and A. H. Abbar, "Removal of COD from Petroleum refinery Wastewater by Electro-Coagulation Process Using SS/Al electrodes," *IOP Conference Series: Materials Science and Engineering*, vol. 870, no. 1, Jun. 2020, Art. no. 012052, https://doi.org/10.1088/1757-899X/870/1/012052.

[17] G. Hayder, M. Z. Ramli, M. A. Malek, A. Khamis, and N. M. Hilmin, "Prediction model development for petroleum refinery wastewater treatment," *Journal of Water Process Engineering*, vol. 4, pp. 1–5, Dec. 2014, https://doi.org/10.1016/j.jwpe.2014.08.006.

[18] C. A. Martinez-Huitle and E. Brillas, "Decontamination of wastewaters containing synthetic organic dyes by electrochemical methods: A general review," *Applied Catalysis B: Environmental*, vol. 87, no. 3, pp. 105–145, Apr. 2009, https://doi.org/10.1016/j.apcatb.2008.09.017.

[19] Y. Yavuz, A. S. Koparal, and U. B. Ogutveren, "Treatment of petroleum refinery wastewater by electrochemical methods," *Desalination*, vol. 258, no. 1, pp. 201–205, Aug. 2010, https://doi.org/10.1016/j.desal.2010.03.013.

[20] L. Yan, H. Ma, B. Wang, Y. Wang, and Y. Chen, "Electrochemical treatment of petroleum refinery wastewater with three-dimensional multi-phase electrode," *Desalination*, vol. 276, no. 1, pp. 397–402, Aug. 2011, https://doi.org/10.1016/j.desal.2011.03.083.

[21] R. H. Salman, "Removal of Manganese Ions (Mn2+) from a Simulated Wastewater by Electrocoagulation/ Electroflotation Technologies with Stainless Steel Mesh Electrodes: Process Optimization Based on Taguchi Approach," *Iraqi Journal of Chemical and Petroleum Engineering*, vol. 20, no. 1, pp. 39–48, Mar. 2019, https://doi.org/10.31699/IJCPE.2019.1.6.

[22] T. Satapanajaru, S. D. Comfort, and P. J. Shea, "Enhancing Metolachlor Destruction Rates with Aluminum and Iron Salts during Zerovalent Iron Treatment," *Journal of Environmental Quality*, vol. 32, no. 5, pp. 1726–1734, 2003, https://doi.org/10.2134/jeq2003.1726.

[23] V. Khandegar and A. K. Saroha, "Electrocoagulation for the treatment of textile industry effluent – A review," *Journal of Environmental Management*, vol. 128, pp. 949–963, Oct. 2013, https://doi.org/10.1016/j.jenvman.2013.06.043.

[24] R. Katal and H. Pahlavanzadeh, "Influence of different combinations of aluminum and iron electrode on electrocoagulation efficiency: Application to the treatment of paper mill wastewater," *Desalination*, vol. 265, no. 1, pp. 199–205, Jan. 2011, https://doi.org/10.1016/j.desal.2010.07.052.

[25] Y. Sun *et al.*, "Electrochemical treatment of chloramphenicol using Ti-Sn/γ-Al2O3 particle electrodes with a three-dimensional reactor," *Chemical Engineering Journal*, vol. 308, pp. 1233–1242, Jan. 2017, https://doi.org/10.1016/j.cej.2016.10.072.

[26] M. Paidar, K. Bouzek, M. Laurich, and J. Thonstad, "Application of a Three-Dimensional Electrode to the Electrochemical Removal of Copper and Zinc Ions from Diluted Solutions," *Water Environment Research*, vol. 72, no. 5, pp. 618–625, 2000, https://doi.org/10.2175/106143000X138201.

[27] S. Yonghui, L. Siming, Y. Ning, and H. Wenjin, "Treatment of cyanide wastewater dynamic cycle test by three-dimensional electrode system and the reaction process analysis," *Environmental Technology*, vol. 42, no. 11, pp. 1693–1702, May 2021, https://doi.org/10.1080/09593330.2019.1677783.

[28] S. T. Kadhum, G. Y. Alkindi, and T. M. Albayati, "Remediation of phenolic wastewater implementing nano zerovalent iron as a granular third electrode in an electrochemical reactor," *International Journal of Environmental Science and Technology*, vol. 19, no. 3, pp. 1383–1392, Mar. 2022, https://doi.org/10.1007/s13762-021-03205-5.

[29] R. Shokoohi *et al.*, "Comparing the performance of the peroxymonosulfate/Mn3O4 and three-dimensional electrochemical processes for methylene blue removal from aqueous solutions: Kinetic studies," *Colloid and Interface Science Communications*, vol. 42, May 2021, Art. no. 100394, https://doi.org/10.1016/j.colcom.2021.100394.

[30] S. Sowmiya, R. Gandhimathi, S. T. Ramesh, and P. V. Nidheesh, "Granular activated carbon as a particle electrode in three-dimensional electrochemical treatment of reactive black B from aqueous solution," *Environmental Progress & Sustainable Energy*, vol. 35, no. 6, pp. 1616–1622, 2016, https://doi.org/10.1002/ep.12396.

[31] S. Tang *et al.*, "Fe3O4 nanoparticles three-dimensional electro-peroxydisulfate for improving tetracycline degradation," *Chemosphere*, vol. 268, Apr. 2021, Art. no. 129315, https://doi.org/10.1016/j.chemosphere.2020.129315.

[32] P. Pourali, M. Fazlzadeh, M. Aaligadri, A. Dargahi, Y. Poureshgh, and B. Kakavandi, "Enhanced three-dimensional electrochemical process using magnetic recoverable of Fe3O4@GAC towards furfural degradation and mineralization," *Arabian Journal of Chemistry*, vol. 15, no. 8, Aug. 2022, Art. no. 103980, https://doi.org/10.1016/j.arabjc.2022.103980.

[33] K. GracePavithra, P. Senthil Kumar, V. Jaikumar, and P. SundarRajan, "A review on three-dimensional eletrochemical systems: analysis of influencing parameters and cleaner approach mechanism for wastewater," *Reviews in Environmental Science and Bio/Technology*, vol. 19, no. 4, pp. 873–896, Dec. 2020, https://doi.org/10.1007/s11157-020-09550-0.

[34] W. Can, H. Yao-Kun, Z. Qing, and J. Min, "Treatment of secondary effluent using a three-dimensional electrode system: COD removal, biotoxicity assessment, and disinfection effects," *Chemical Engineering Journal*, vol. 243, pp. 1–6, May 2014, https://doi.org/10.1016/j.cej.2013.12.044.

[35] X. Li, C. Wang, Y. Qian, Y. Wang, and L. Zhang, "Simultaneous removal of chemical oxygen demand, turbidity and hardness from biologically treated citric acid wastewater by electrochemical oxidation for reuse," *Separation and Purification Technology*, vol. 107, pp. 281–288, Apr. 2013, https://doi.org/10.1016/j.seppur.2013.01.008.

[36] N. R. Neti and R. Misra, "Efficient degradation of Reactive Blue 4 in carbon bed electrochemical reactor," *Chemical Engineering Journal*, vol. 184, pp. 23–32, Mar. 2012, https://doi.org/10.1016/j.cej.2011.12.014.

[37] L. Correia-Sa *et al.*, "A Three-Dimensional Electrochemical Process for the Removal of Carbamazepine," *Applied Sciences*, vol. 11, no. 14, Jan. 2021, Art. no. 6432, https://doi.org/10.3390/app11146432.

[38] K.-W. Jung, M.-J. Hwang, D.-S. Park, and K.-H. Ahn, "Combining fluidized metal-impregnated granular activated carbon in three-dimensional electrocoagulation system: Feasibility and optimization test of color and COD removal from real cotton textile wastewater," *Separation and Purification Technology*, vol. 146, pp. 154–167, May 2015, https://doi.org/10.1016/j.seppur.2015.03.043.

[39] E. Gengec, M. Kobya, E. Demirbas, A. Akyol, and K. Oktor, "Optimization of baker's yeast wastewater using response surface methodology by electrocoagulation," *Desalination*, vol. 286, pp. 200–209, Feb. 2012, https://doi.org/10.1016/j.desal.2011.11.023.

[40] J. B. Parsa, H. R. Vahidian, A. R. Soleymani, and M. Abbasi, "Removal of Acid Brown 14 in aqueous media by electrocoagulation: Optimization parameters and minimizing of energy consumption," *Desalination*, vol. 278, no. 1, pp. 295–302, Sep. 2011, https://doi.org/10.1016/j.desal.2011.05.040.

[41] D. Kumar and C. Sharma, "Remediation of Pulp and Paper Industry Effluent Using Electrocoagulation Process," *Journal of Water Resource and Protection*, vol. 11, no. 3, pp. 296–310, Mar. 2019, https://doi.org/10.4236/jwarp.2019.113017.

[42] D. S. Ibrahim, P. S. Devi, and N. Balasubramanian, "Electrochemical Oxidation Treatment of Petroleum Refinery Effluent," *International Journal of Scientific and Engineering Research*, vol. 4, no. 8, pp. 1–5, Jan. 2013, https://doi.org/10.14299/00000.

[43] M. S. Secula, A. Vajda, L. Hagiu-Zaleschi, B. Cagnon, F. Warmont, and I. Mamaliga, "Iron(II)-Impregnated Activated Carbon Composites Applied as Fenton-like Catalysts for Degrading Persistent Organic

Compounds," in *15th International Conference on Environmental Science and Technology*, Rhodes, Greece, Sep. 2017.

[44] U. Balasubramani, R. Venkatesh, S. Subramaniam, G. Gopalakrishnan, and V. Sundararajan, "Alumina/activated carbon nano-composites: Synthesis and application in sulphide ion removal from water," *Journal of Hazardous Materials*, vol. 340, pp. 241–252, Oct. 2017, https://doi.org/10.1016/j.jhazmat.2017.07.006.

[45] A. Kolics, J. C. Polkinghorne, and A. Wieckowski, "Adsorption of sulfate and chloride ions on aluminum," *Electrochimica Acta*, vol. 43, no. 18, pp. 2605–2618, Jun. 1998, https://doi.org/10.1016/S0013-4686 (97)10188-8.

[46] R. Keyikoglu, O. T. Can, A. Aygun, and A. Tek, "Comparison of the effects of various supporting electrolytes on the treatment of a dye solution by electrocoagulation process," *Colloid and Interface Science Communications*, vol. 33, Nov. 2019, Art. no. 100210, https://doi.org/ 10.1016/j.colcom.2019.100210.

[47] C. J. Israilides, A. G. Vlyssides, V. N. Mourafeti, and G. Karvouni, "Olive oil wastewater treatment with the use of an electrolysis system," *Bioresource Technology*, vol. 61, no. 2, pp. 163–170, Aug. 1997, https://doi.org/10.1016/S0960-8524(97)00023-0.

[48] S. H. Lin, C. T. Shyu, and M. C. Sun, "Saline wastewater treatment by electrochemical method," *Water Research*, vol. 32, no. 4, pp. 1059–1066, Apr. 1998, https://doi.org/10.1016/S0043-1354(97)00327-8.

[49] A. G. Vlyssides, C. J. Israilides, M. Loizidou, G. Karvouni, and V. Mourafeti, "Electrochemical treatment of vinasse from beet molasses," *Water Science and Technology*, vol. 36, no. 2, pp. 271–278, Jan. 1997, https://doi.org/10.1016/S0273-1223(97)00398-3.

[50] G. Varank, H. Erkan, S. Yazycy, A. Demir, and G. Engin, "Electrocoagulation of Tannery Wastewater using Monopolar Electrodes: Process Optimization by Response Surface Methodology," *International Journal of Environmental Research*, vol. 8, no. 1, pp. 165–180, Jan. 2014, https://doi.org/10.22059/ijer.2014.706.

[51] K.-W. Jung, M.-J. Hwang, D.-S. Park, and K.-H. Ahn, "Performance evaluation and optimization of a fluidized three-dimensional electrode reactor combining pre-exposed granular activated carbon as a moving particle electrode for greywater treatment," *Separation and Purification Technology*, vol. 156, pp. 414–423, Dec. 2015, https://doi.org/ 10.1016/j.seppur.2015.10.030.

[52] J. A. G. Gomes *et al.*, "Arsenic removal by electrocoagulation using combined Al–Fe electrode system and characterization of products," *Journal of Hazardous Materials*, vol. 139, no. 2, pp. 220–231, Jan. 2007, https://doi.org/10.1016/j.jhazmat.2005.11.108.

[53] M. El-Naas, A.-Z. Sulaiman, and A. Al-Lobaney, "Treatment of petroleum refinery wastewater by continuous electrocoagulation," *International Journal of Engineering Research & Technology*, vol. 2, no. 10, pp. 2144–2150, Jan. 2013.

[54] L. Wei, S. Guo, G. Yan, C. Chen, and X. Jiang, "Electrochemical pretreatment of heavy oil refinery wastewater using a three-dimensional electrode reactor," *Electrochimica Acta*, vol. 55, no. 28, pp. 8615–8620, Dec. 2010, https://doi.org/10.1016/j.electacta.2010.08.011.